Evaluating the features of interdigital neuroma using 3-Tesla magnetic resonance imaging

Tugrul Ormeci[1], Olcay Güler[2], Melih Malkoc[3], Nurullah Kaya[4], Mehmet Isyar[5], Aslı Cakir[6], Selva Sen[7], Mahir Mahiroglulları[2]

[1] Medipol University, Faculty of Medicine, Department of Radiology, Turkey
[2] Memorial Şişli Hospital, Department of Orthopedics and Traumatology, Turkey
[3] European University of Lefke, Faculty of Health Science, Turkey
[4] Koç University, Faculty of Medicine, Department of Radiology, Turkey
[5] Acibadem Kadıköy Hospital, Department of Orthopedics and Traumatology, Turkey
[6] Medipol University, Faculty of Medicine, Department of Medical Pathology, Turkey
[7] Medipol University, Faculty of Medicine, Department of Anatomy, Turkey

SUMMARY

Interdigital neuroma is an entrapment neuropathy of the interdigital nerve. Previously, studies on interdigital neuroma were done with 1 Tesla Magnetic Resonance Imaging and more often 1.5 Tesla Magnetic Resonance Imaging. We used 3 Tesla Magnetic Resonance Imaging in our study and we did not encounter as much as we know about the study with 3 Tesla Magnetic Resonance Imaging in the literature. Between 2013 and 2019, the 3 Tesla Magnetic Resonance Imaging results of 39 consecutive surgically-confirmed interdigital neuromas and patients' files were retrospectively evaluated. The soft tissue surrounding the prominent interdigital nerve "target sign" were assessed. Spearman's rho, Pearson's correlation tests, and Mann-Whitney U-tests were used. Of the 39 cases (mean transverse dimension = 4.64 mm), 35 (89.7%) were hypointense on T1-weighted sequencing, 34 were intermediate (87.1%) on short tau inversion recovery sequencing, and 29 (74.3%) had slightly-moderately enhanced neuromas on post-contrast spectral presaturation with inversion recovery sequences. A statistically significant negative relationship was found between contrast enhancement and disease duration (p = 0.020). On short tau inversion recovery or spectral presaturation with inversion recovery series, the intralesional nerve view "target sign" was observed in 23 (58.98 %) of 39 neuromas. This is the first study in the literature with 3 Tesla Magnetic Resonance Imaging that shows the visual characteristics of interdigital neuroma and its possible contribution to the diagnosis of the disease.

Key words: Morton neuroma – Interdigital neuroma – 3-Tesla MRI – Metatarsalgia – Foot pain

Corresponding author:
Tugrul Ormeci. Medipol University, Faculty of Medicine, Department of Radiology, østanbul, Turkey. Address: Medipol Mega Hastaneler Kompleksi, Radyology Department, TEM Avrupa Otoyolu Göztepe çıkışı No:1 Bağcılar 34214 østanbul/Turkey. Phone: +90 212 4607295; Fax: +90 212 4607050. E-mail: ormecitugrul@gmail.com Orcid ID: 0000-0001-8532-4917.

Submitted: September 15, 2022. **Accepted:** November 7, 2022

https://doi.org/10.52083/OLLN3191

ABBREVIATIONS

MRI, Magnetic Resonance Imaging

SPIR, Spectral Presaturation with Inversion Recovery

STIR, Short Tau Inversion Recovery

T1W, T1-weighted

TSE, Turbo Spin Echo

US, Ultrasonography

INTRODUCTION

Interdigital neuroma, widely known as Morton's neuroma, is an entrapment neuropathy of the interdigital nerve, and is more frequently diagnosed in middle-aged women (Wu, 1996). Specific physical examination findings (such as Mulder's sign, Tinel's sign, etc.) used in interdigital neuroma diagnosis was defined in the literature and some authors state that the diagnosis can be made using both clinical and physical examination findings (Zanetti et al., 1997a, b; Shapiro et al., 1995; Levine et al., 1998). MRI (magnetic resonance imaging) and US (ultrasonography) are used for the possibility of comorbid conditions or for legal reasons, or to confirm the initial diagnosis (Zanetti et al., 1997a; Biasca et al., 1999). In cases of interdigital neuroma, an increased transverse relaxation time (T2) signal, greater calibration, and increased contrast uptake may be seen on MRI due to the affected interdigital nerve. Some authors have also reported a relationship between neuroma and the interdigital nerve (Simmons, 2008; Waizy et al., 2010). The term "target sign" is used for central hypointense and peripheral hyperintense-looking round tumors derived from neural tissue (Bhargava et al., 1997). Although this sign is highly suggestive of peripheral nerve sheath tumors like as neurofibroma, in this study we observed the slightly edematous interdigital nerve and surrounding soft-tissue view "target sign" in some of our interdigital neuroma cases (Fig. 1). Observing the affected nerve using 3T (Tesla), MRI can be interpreted as a positive indicator in the diagnosis of interdigital neuroma. Previously, studies on interdigital neuroma were done with 1T MRI and more often 1.5T MRI (Zanetti et al., 1997a; Lee et al., 2007; Williams et al., 1997; Erickson et al., 1991; Bencardino et al., 2000). We used 3T MRI in our study and we did not encounter as much as we know about the study with 3T MRI in the literature.

The aim of this study was to evaluate the visual characteristics of interdigital neuroma with 3T MRI and its contribution to diagnosis.

MATERIALS AND METHODS

Study population

Approval for this study was obtained from the local ethics committee (number and date: 108400987-173/2015). Between 2013 and 2019, the 3T MRI results of 39 consecutive surgically-confirmed interdigital neuromas in 30 patients

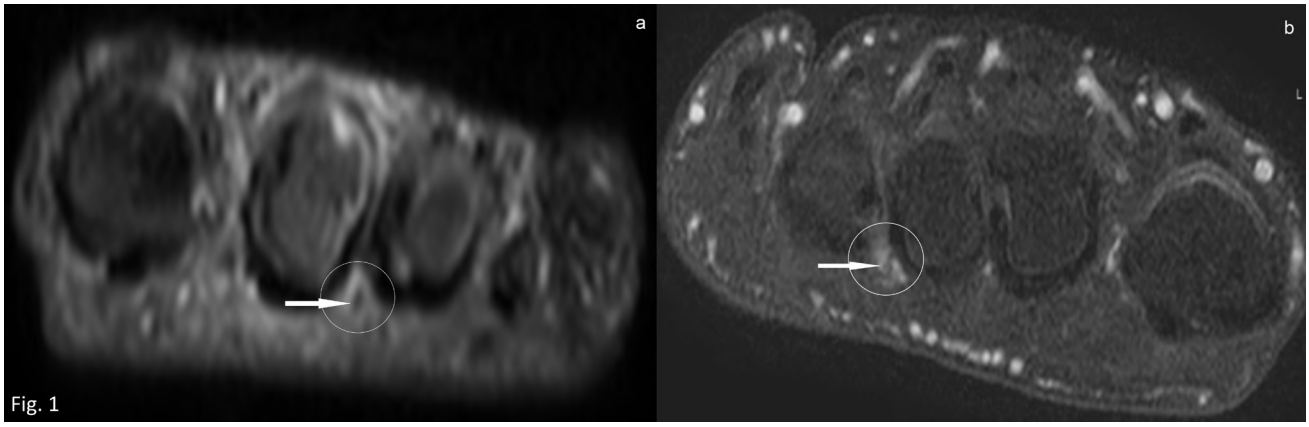

Fig. 1

Fig. 1.- Magnetic resonance imaging view of the "target sign'' and its histopathological reflection. (**a)** The "target sign'' in 44-year-old man with interdigital neuroma. The prominent and mildly-hyperintense interdigital nerve (arrow) can be seen in the 2nd web space on the coronal short tau inversion recovery (STIR) image. (**b)** A 51-year-old woman with interdigital neuroma. On the coronal post-contrast spectral presaturation with inversion recovery (SPIR) image, a moderately-contrasted soft-tissue formation (circled) surrounding the slightly visible interdigital nerve (arrow) can be seen within the 3rd web space: "target sign''.

were retrospectively evaluated. Of the 30 included patients, 18 (60%) were female and 12 (40%) were male. Nine cases had lesions in two web spaces (the 2nd and 3rd web spaces), and a total of 39 interdigital neuromas were included in the study. The mean age of the neuroma patients was 40.77 years (range, 21-71 years). Patients who were treated conservatively for forefoot pain but did not respond to these treatments were included in the study. In the evaluation based on both physical and MRI examinations, patients diagnosed with interdigital neuroma underwent surgery, and the diagnosis was confirmed histopathologically. The interdigital neuromas were reviewed independently by two radiologists experienced in the musculoskeletal system. We excluded cases with a medical history of previous surgery on the same foot, trauma occurring at least 6 months prior, any congenital deformity of the foot, diabetes, and any vascular disease of the foot.

Consequently, The 3T MRI features of 39 interdigital neuromas that were diagnosed histopathologically were retrospectively evaluated.

Magnetic Resonance Imaging

MRI studies were conducted with a 3T scanner (MR Systems Achieva Release 3.2.3.1, Philips Medical Systems, Holland) using a sense foot/ankle coil with eight channels. The routine protocol we used for interdigital neuroma is described in supplementary material. Ovoid or round mass lesions between the metatarsal heads with substantial demarcation were investigated for interdigital neuroma, as described in the literature (Gougoulias et al., 2019; Bhatia and Thomson, 2020). If a lesion was present, the location, dimension, signal characteristics on T1W, STIR (Short Tau Inversion Recovery), and contrast series, and the duration time of the disease as well as the relationship among these factors were evaluated. The lesion conspicuity was evaluated qualitatively for T1W, STIR and post contrast sequences, as it was done in the literature (Terk et al., 1993; Lee et al., 2007; Williams et al., 1997; Erickson et al., 1991). An accumulation of fluid greater than 3 mm in the transverse plane in the intermetatarsal bursa has been described as bursitis (Zanetti et al., 1997b). In addition to these factors, coexisting pathologies, such as intermetatarsal bursal fluid accumulation (bursitis), were also assessed. The target sign, which is defined as the soft tissue appearance described as the hypointense centrally and hyperintense peripherally, was examined. The relationship between the features of the lesion and target sign were assessed. All the neuromas were reviewed by both radiologists to determine the diagnostic value of the 3T MRI sequences. In disputed cases, a consensus was reached after a mutual review of the data.

Statistical Analysis

Descriptive statistical methods were used during the data review. Spearman's rho and Pearson's correlation tests were used to define the correlation between the factors. To define the significant differences, the chi-square and Mann-Whitney U tests were used. The results were reviewed with regard to the 95% confidence interval and 5% significance level. SPSS Statistics for Windows version 22.0 (IBM Corp., Armonk, NY, USA) and Microsoft Excel 2007 (Microsoft, Redmond, WA, USA) were used for the statistical analysis.

RESULTS

Of the 30 included patients, the mean duration of the disease was 31.95 months (range, 1-120 months). Most of the lesions were in the 3rd intermetatarsal space. The mean neuroma size was 4.64 mm (range, 2.70-9 mm). If we removed a single large 9 mm lesion, the average neuroma size was 4.53 mm. Only one of 39 neuromas could not be detected on MRI. The diagnostic accuracy was found to be 97.4%. No correlation was detected between disease duration and the age of the patient ($r= 0.086$, $p=0.610$), and there was no statistically significant correlation between the neuroma size measured with MRI and the disease duration ($r = 0.024$, $p = 0.890$). Eight of the 39 lesions (20.5%) had intermetatarsal bursitis, and their mean size was 3.68 mm (Table 1). 46% (21 cases) of interdigital neuromas had accompanying intermetatarsal bursal effusion. It was observed that neuromas exceeded the intermetatarsal line by an average of 3.20 mm (range, 1.2-5.5 mm).

Table 1. The features of interdigital neuroma.

		Total	1st Web N (%)	2nd Web N (%)	3rd Web N (%)	Duration Time (months)	
Interdigital Neuroma		39 (in 30 pts)	1 (2.57%)	10 (25.64%)	28 (71.79%)		
Sex	Female	25 (64.1%)	1 (4%)	6 (24%)	18 (72%)		
	Male	14 (35.9%)	0 (0%)	4 (28.6%)	10 (71.4%)		
I.N. size (mm)		4.64 (2.7-9)	9	4.58 (3.2-7.3)	4.51 (2.7-7)		0.23**
Bursitis (mm)		2.77 (1.3-5.3)	3.6	3.07 (2.1-3.7)	2.66 (1.3-5.3)		0.32**
''Target Sign''	-	16 (41.02%)	1(6.25%)	5 (31.25%)	10 (62.5%)	40.94 (1-120)	0.35*
	+	23 (58.98%)	0 (0%)	5 (21.73%)	18 (78.26%)	25.69 (1-96)	
T1W im		4 (10.26)	0 (0%)	0 (0%)	4 (100%)	29.5 (1-96)	0.42*
T1W hypo		35 (89.74%)	1 (2.9%)	10 (28.6%)	24 (68.6%)	32.23 (1-120)	

*: Statistical difference between the 1st, 2nd and 3rd web spaces (*Chi Square Test*).
**: Statistical difference between 2nd and 3rd Web spaces (*Mann Whitney U Test*).
I.N.: Interdigital neuroma, im: intermediate, hypo: hypointense.

The target sign view was observed in 23 (59%) of the 39 lesions; it could not be detected in 16 lesions (41%). Only 5 out of the 23 target sign views were seen in the 2nd intermetatarsal web space; the rest were in the 3rd intermetatarsal web space. A statistically significant relationship between the target sign and disease duration or the lesion size was not detected (disease duration with target sign: r = −0.195, p = 0.230; size in MRI with target sign: r = 0.053, p = 0.747, respectively). The mean duration time of 16 cases without a target sign is 40.94 months (range,1-120 months); the mean duration time of the 23 cases with a target sign is 25.69 months (range, 1-96 months).

Among the total cases, 35 (89.7%) were hypointense and 4 (10.3%) had an intermediate signal on the T1W sequences. On the STIR sequences,

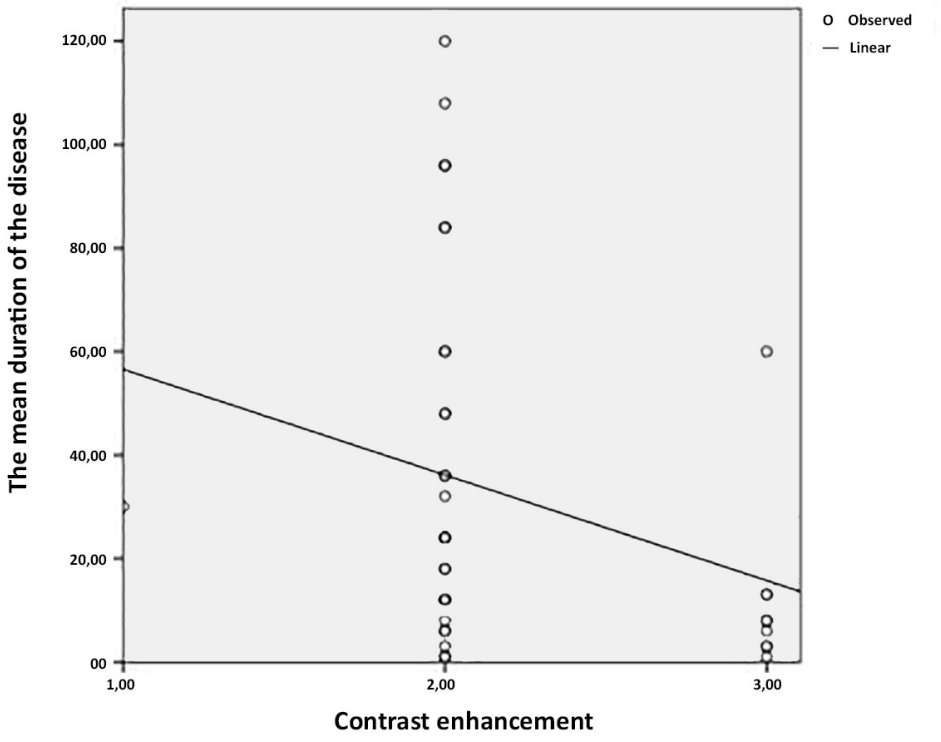

Fig. 2.- The relationship between the mean duration of the disease and contrast enhancement.

34 (87.1%) cases were intermediate, 1 (2.6%) was hypointense, and 4 (10.3%) were hyperintense. There were 29 (74.3%) cases which were slightly-moderately enhanced and 9 (23.1%) cases with a significantly enhanced neuroma on the post-contrast series. Contrast enhancement was not detected in one case. The disease duration for the lesions that were slightly-moderately enhanced was 37.97 months (standard deviation 36.59; range, 1-120 months); for significantly enhanced lesions, it was 12.78 months (standard deviation 18.21; range, 1-60 months). The disease duration difference for contrast enhancement was statistically significant. A statistically significant negative relationship was found between contrast enhancement and disease duration ($r = -0.37$; $p = 0.020$). Disease duration is shorter as the contrast enhancement increases (Fig. 2).

For the T1W sequences, the disease duration for the lesions visible at the intermediate signal level was 29.5 months (range, 1-96 months); however, this duration increased to 32.23 months (range, 1-120 months) when the signal was hypointense.

When the diagnostic benefits (lesion identification level) of the T1, STIR, and post-contrast SPIR (Spectral Presaturation with Inversion Recovery) sequences were assessed, 26 (66.7%) out of a total of 39 lesions were best viewed on the T1 sequences, 6 (15.4%) were best viewed on the STIR sequences, and 7 (17.9%) were best viewed on the post-contrast SPIR sequences.

DISCUSSION

Interdigital neuroma is one of the most common causes of forefoot pain (Zanetti et al., 1997a, b). In the evaluation based on both physical and MRI examinations, 30 patients underwent surgery and the condition was confirmed histopathologically (39 interdigital neuromas in 30 patients). It was observed that 1 of these 39 cases could not be detected on MRI because of the presence a small, double lesion. With this result, the diagnostic accuracy was found to be 97.4%.

In our study, interdigital neuroma was mainly diagnosed within the 3rd web space, and our results were consistent with those reported in previous studies in the literature (Gougoulias et al., 2019; Choi et al., 2021). In the literature average size of neuroma was reported 7.5 ± 0.7 mm (Samaila et al., 2021). Ruiz et al. (2019) reported that the transverse axis of lesion was 5.5 mm. We found that the mean dimension was 4.64 mm (range, 2.7-9 mm). If we removed a single large 9 mm lesion, the average neuroma size was 4.53 mm. It is possible to detect small lesions with 3T MRI due to the increased resolution. Bencardino et al. (2000) reported that the mean transverse diameter of symptomatic neuromas was 5.3 mm (standard deviation, 2.14), whereas that the mean transverse diameter of asymptomatic neuromas was 4.1 mm (standard deviation, 1.75). Sharp et al. (2003) stated that interdigital neuromas smaller than 6 mm can also show clinical symptoms. In our study, we found the mean size of the symptomatic lesion was even smaller (4.64 mm).

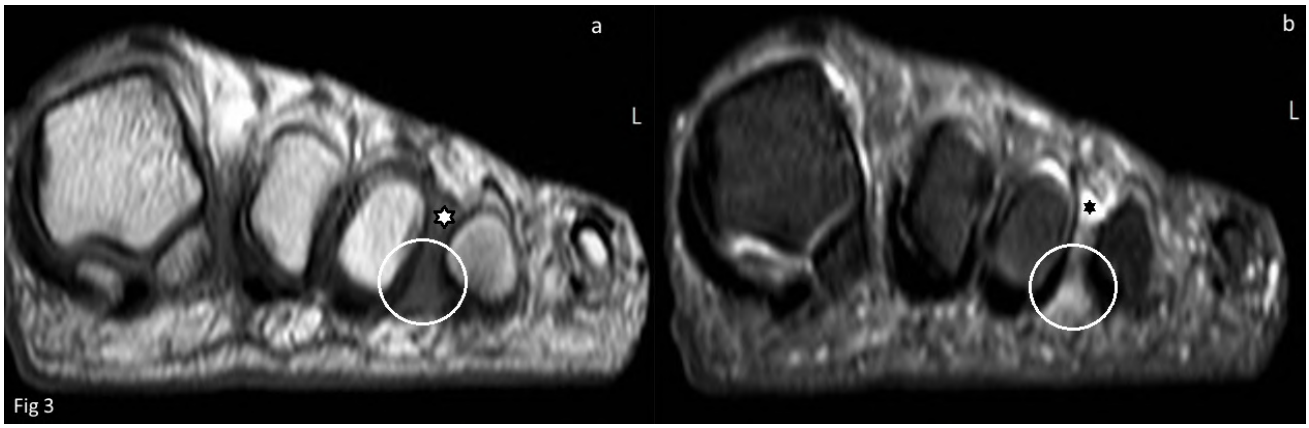

Fig. 3.- An interdigital neuroma with intermetatarsal bursal effusion. A 48-year-old man with interdigital neuroma. On images **(a)** coronal Turbo spin echo (TSE) T1, and **(b)** coronal STIR, interdigital neuroma (circled) is visible in the 3rd web space as T1 hypointense and STIR intermediate. An intermetatarsal bursal effusion is also prominent (asterisk*) in the adjacent superior area.

In our study, 46% (21 cases) of our interdigital neuroma cases had accompanying intermetatarsal bursal effusion (Fig. 3). However, bursal effusion wider than 3 mm was only present in 8 cases (20.5%) and the mean size of the coronal plane was 3.68 mm.

If a lesion is sufficiently large, a significant plantar extension pass across the intermetatarsal line is seen, which allows for an easier diagnosis. In our study, it was observed that neuromas exceeded the intermetatarsal line by an average of 3.20 mm (range, 1.2-5.5 mm). However, if the lesion does not exceed the intermetatarsal line, diagnosis can be difficult. In small-dimensioned neuromas, the obliteration of the hyperintense signal arising from the fatty tissue located in the conic-shaped space (along with the nerve) by the lesion can serve as a warning sign (Fig. 4).

Interdigital neuroma reportedly displays different signal characteristics in different magnetic field strengths, and the diagnostic benefit of the sequences that are used also varies. George et al. (2005) reported that STIR is the most sensitive sequence in their 1-Tesla (1T) study. However, studies conducted by Zanetti et al. (1T), Lee et al. (1.5T), Bencardino et al. (1.5T), Williams et al. (1.5T), and Erickson et al. (1.5T) all reported the T1W sequence to be the most sensitive (Zanetti et al., 1997a, b; Lee et al., 2007; Williams et al., 1997; Erickson et al., 1991; Bencardino et al., 2000). Furthermore, Terk et al. (1993), George et al. (2005), and Unger et al. (1992) also reported the beneficial use of contrasted series. However, Zanetti et al. (1997a), Lee et al. (2007), and Williams et al. (1997) did not report the superiority of post-contrast T1 images over other sequences used for diagnosis.

In our study, in comparison to the adjacent fat planes, 35 (89.7%) of the neuroma cases provided a hypointense signal on the T1W sequences, in 34 cases the signals were intermediate (87.1%) on the STIR sequences, and in 38 (97.4%) cases the signals were slightly-moderately enhanced on the post-contrast series. Based on these findings, we can say that, in general, interdigital neuromas are viewed as a hypointense signal on T1W, an intermediate signal on the STIR sequences, and a slightly-moderately enhanced signal on the post-contrast series with 3T MRI. Out of a total of 39 lesions, 26 (66.7%) were best viewed on the T1 sequences, 6 (15.4%) were best viewed on STIR sequences, and 7 (17.9%) were best viewed on the post-contrast SPIR sequences. As detailed, the T1W sequences were the most diagnostically beneficial sequences. However, a detailed review of the STIR and post-contrast SPIR sequences may assist in clinical decision making for the diagnosis of small lesions, especially if other or accompanying lesions are causing metatarsalgia.

In the literature, general expressions about the signal properties of interdigital neuroma in T1W and T2W sequences have been used. T2W sequences were taken as non-fat-saturated in some of the studies and as fat saturated T2W or as STIR

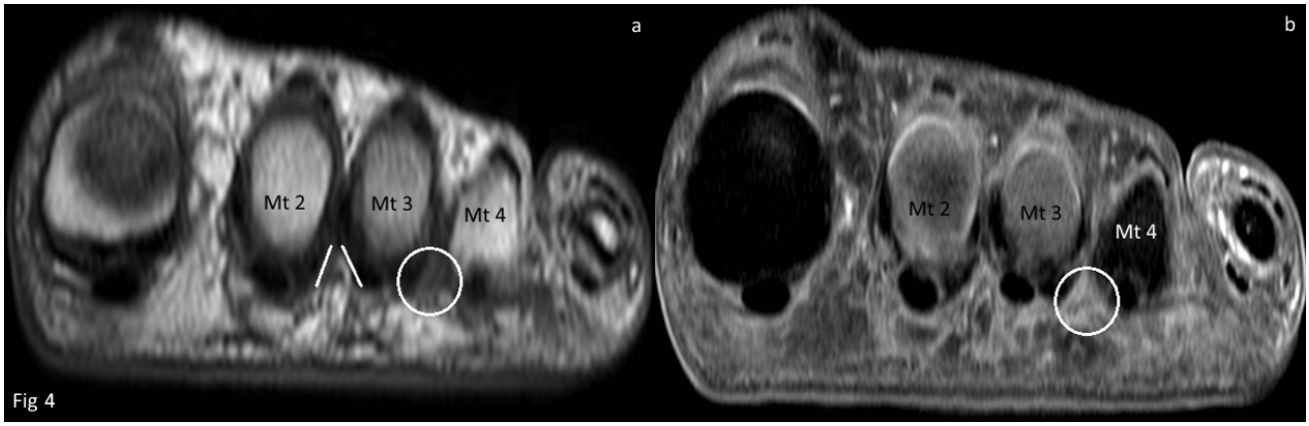

Fig. 4.- The fatty tissues are obliterated by the interdigital neuroma. A 37-year-old woman with metatarsalgia. On images **(a)** coronal TSE T1, and **(b)** coronal post-contrast SPIR, straight lines indicate the conical area within the 2nd web space formed by deep transverse metatarsal ligaments, and the dorsal and plantar interosseous tendons. This hyperintense area due to fatty tissue can be easily identified. In the 3rd web space, fatty tissues are obliterated by the interdigital neuroma (circled).

in other studies. In their 1T MRI study, Zanetti et al. (1997a) defined the interdigital neuroma signal as low in all the T1W and T2W series and generally high (9/14) in the STIR sequence. Sharp et al. found that the interdigital neuroma signal was low or intermediate (isointense with muscle) in the T1W series; in their study with 1.5T MRI, they reported that the T2W findings were highly variable and the T2W signal increased in 18/24 lesions (Sharp et al., 2003).

In musculoskeletal examinations in 3T MRI systems, the T1 value ranges between 10-30%, which is higher than it is in 1.5T MRI systems (Mosher, 2006). Again, as the magnetic field strength of the device increases, the T2 values of the tissues remain constant or decrease slightly (Bottomley et al., 1984). If we ignore the effects of time on lesions, in our study, the lesions were mostly hypointense on the T1W series (35/39) and intermediate on the STIR sequence (34/39), probably due to these effects.

Betts et al. (2003) reported that, due to the inflammatory response and fluid accumulation in the early period, there is echo enhancement in the distal portion of the lesion on US; however, as the disease duration increases, the lesion becomes more solid and difficult to see distinctly from the surrounding structures. Using the same mechanism, in our study, although the relationship between disease duration and T1 signal was not statistically significant, the mean duration of the lesions seen in the intermediate signal in the T1W series was 29.5 months; this time increased to 32.2 months when the signal returned to hypointense. (It should be noted that the duration of the disease is obtained from the patient's medical history, thus the information might not be reliable). This is in accordance with the fact that fibrosis increases with the progression of the disease and, thus, hypointensity becomes more prominent (Fig. 5). Contrast enhancement, which is more common in the early stages of the disease, decreases due to fibrosis as the disease progresses.

The normal plantar digital nerve calibration is approximately 1-2 mm at the level of the metatarsal head (Nissen, 1948). In MRI images, the hyperintense signal on the STIR sequence is secondary to edema, and increased calibration of the nerve can be observed. Calibration increases with long-term nerve fiber degeneration, and excessive intraneural and juxtaneural reparative fibrosis (Wu, 1996). However, our cases showed no significant calibration increase in the nerve. It has been reported that the best diagnosis method is the visibility of the digital nerve within the lesion (Simmons, 2008). Waizy et al. (2010) argued that to diagnose interdigital neuroma, the lesion should be viewed within the neurovascular bundle. The term, target sign, is used for central hypointense and peripheral hyperintense-looking round tumors (peripheral nerve sheath tumors, such as neurofibroma) derived from neural tissue (Bhargava et al., 1997). We found that, on the post-contrast series and even on the STIR images in some of the cases, the

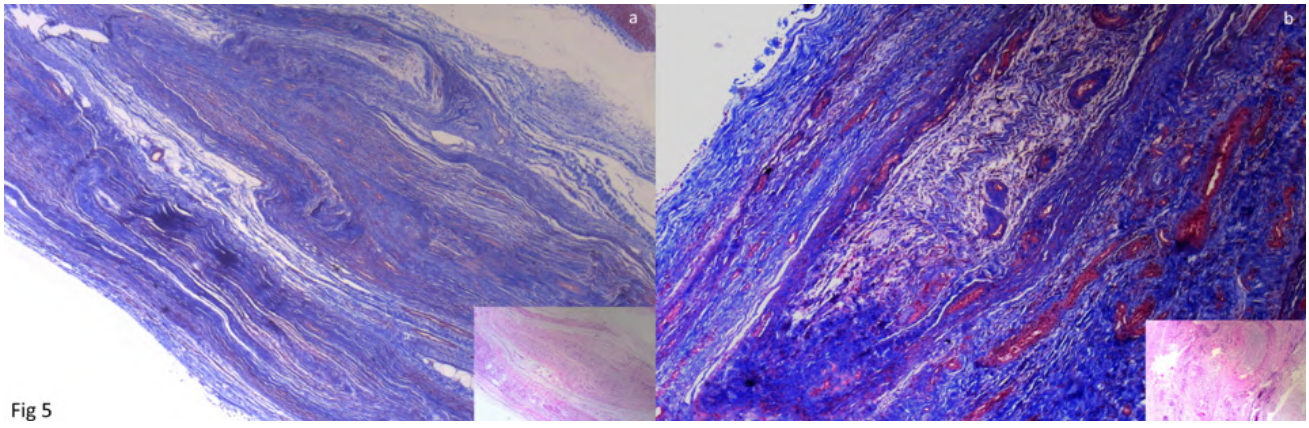

Fig. 5.- Pathological specimens of two different interdigital neuroma patients. First case (54-year-old woman). **(a)** has an earlier lesion than the second one (28-year-old woman). **(b)** Fibrosis and the connective tissue surrounding the nerve are more prominent in b than a. Marked fibrosis is stained darker blue with Masson Trichrome staining in b than a. (a, b = x40 MT; a-inset, b-inset = x40 HE).

hypointense nerve in the surrounding enhanced and hyperintense (to varying degrees) soft tissue makes the appearance of the target sign (Fig. 1). This finding was observed in 23 (59%) of the 39 neuromas.

Some studies claimed that a contrasted series is diagnostically useful (Terk et al., 1993; George et al., 2005; Unger et al., 1992). Lee et al. (2007) also stated that contrast-enhanced series and T2W images are not essential for diagnosis, but are useful in differential diagnosis. Santiago et al. (2018) reported that, if clinically supported, a contrast enhanced series is not required for a reliable diagnosis of interdigital neuroma. We think that the target sign can increase the reliability of the diagnosis of interdigital neuroma by showing the nerve inside the lesion. At this point, and in addition to the information presented above, we believe that the post-contrast series can be useful.

Conservative and surgical treatment options are available in the treatment of interdigital neuroma. Conservative treatments such as shoe modification, use of insoles, and administration of anti-inflammatory drugs, can be tried in the early stages of the disease. Percutaneous therapies can be used, such as injections of local anesthetics, with or without steroids, or of alcohol (Samaila et al., 2020; Sato et al., 2022). Some studies reported that the size of the lesion will affect the treatment option (Biasca et al., 1999; Makki et al., 2012; Park et al., 2018). Surgical treatment is indicated in cases that do not respond to any other treatments. Neurectomy can be performed with a dorsal or plantar approach. Surgical treatment success rates range from 88-94% (Valisena et al., 2018). However, surgical treatment may not always yield a positive result. This failure may be due to the incorrect indication for surgery or to excising the asymptomatic interdigital nerve (Weinfeld and Myerson, 1996). This reinforces the importance of making a correct diagnosis. When the lesion is small, 3T MRI can be used diagnose it early due to increased resolution.

This study has some limitations. The retrospective nature of the study design is the primary limitation. The sensitivity of our study was based on histopathologically confirmed cases, but due to ethical values and legal reasons, the sensitivity could not be calculated because the true-negative ratio was unknown. While we consider that the target sign can be seen with 1.5T MRI, it might be better evaluated with 3T MRI due to increased resolution. However, we could not encounter any article in the literature that assessed the appearance of the target sign with 1.5T MRI in interdigital neuroma.

CONCLUSION

In conclusion, to the best of our knowledge, this is the first study in the literature on 3T MRI that shows the visual characteristics of interdigital neuroma and its possible contribution to the diagnosis of the disease. Our results show that the most useful sequence in diagnosis appears to be the T1W sequence in 3T MRI, and that the identification of the nerve within the soft tissue, the appearance of the target sign, can guide the diagnosis. The high-resolution images obtained via 3T MRI mean that it becomes much easier to detect small lesions, which are potential causes of metatarsalgia. Diagnosing the lesions when the lesion sizes are smaller in the early period of interdigital neuroma may increase the chances of treating patients without surgery. Thus, early diagnosis can help manage the treatment of interdigital neuroma.

Patient Confidentiality and Consent to Publication: This study have been performed according to the Declaration of Helsinki.

REFERENCES

BENCARDİNO J, ROSENBERG ZS, BELTRAN J, LİU X, MARTY-DELFAUT E (2000) Morton's neuroma: is it always symptomatic? *Am J Roentgenol*, 175(3): 649-653.

BETTS RP, BYGRAVE CJ, JONES S, SMİTH TWD, FLOWERS MJ (2003) Ultrasonic diagnosis of Morton's neuroma: a guide to problems, pointers, pitfalls and prognosis. *The Foot*, 13: 92-99.

BHARGAVA R, PARHAM DM, LASATER OE, CHARİ RS, CHEN G, FLETCHER BD (1997) MR imaging differentiation of benign and malignant peripheral nerve sheath tumors: use of the target sign. *Pediatr Radiol*, 27: 124-129.

BHATİA M, THOMSON L (2020) Morton's neuroma–current concepts review. *J Clin Orthop Trauma,* 11(3): 406-409.

BİASCA N, ZANETTİ M, ZOLLİNGER H (1999) Outcomes after partial neurectomy of Morton's neuroma related to preoperative case histories, clinical findings and findings in magnetic resonance imaging scans. *Foot Ankle Int,* 20: 568-575.

BOTTOMLEY PA, FOSTER TH, ARGERSİNGER RE, PFEİFER LM (1984) A review of normal tissue hydrogen NMR relaxation times and relaxation mechanisms from 1-100 MHz: dependence on tissue type, NMR frequency, temperature, species, excision, and age. *Med Phys*, 11: 425-448.

CHOİ JY, LEE HI, HONG WH, SUH JS, HUR JW (2021) Corticosteroid injection for Morton's interdigital neuroma: a systematic review. *Clin Orthop Surg*, 13(2): 266.

ERİCKSON SJ, CANALE PB, CARRERA, GF, JOHNSON JE, SHEREFF MJ, GOULD JS, HYDE JS, JESMANOWİCZ A (1991) Interdigital (Morton) neuroma: high-resolution MR imaging with a solenoid coil. *Radiology*, 181(3): 833-836.

GEORGE VA, KHAN AM, HUTCHİNSON CE, MAXWELL HA (2005) Morton's neuroma: the role of MR scanning in diagnostic assistance. *The Foot*, 15: 14-16.

GOUGOULİAS N, LAMPRİDİS V, SAKELLARİOU A (2019) Morton's interdigital neuroma: instructional review. *EFORT open reviews*, 4(1): 14-24.

LEE MJ, KİM S, HUH YM, SONG, HT, LEE, SA, LEE JW, SUH JS (2007) Morton neuroma: evaluated with ultrasonography and MR imaging. *Korean J Radiol*, 8(2): 148-155.

LEVİNE SE, MYERSON MS, SHAPİRO PP, SHAPİRO SL (1998) Ultrasonographic diagnosis of recurrence after excision of an interdigital neuroma. *Foot Ankle Int*, 19(2): 79-84.

MAKKİ D, HADDAD BZ, MAHMOOD Z, SHAHİD MS, PATHAK S, GARNHAM I (2012) Efficacy of corticosteroid injection versus size of plantar interdigital neuroma. *Foot Ankle Int,* 33: 722-726.

MOSHER TJ (2006) Musculoskeletal imaging at 3T: current techniques and future applications. *Magn Reson Imaging Clin N Am,* 14: 63-76. Review.

NİSSEN KI (1948) Plantar digital neuritis: Morton's metatarsalgia. *J Bone and Joint Surg (Br)*, 30: 84-94.

PARK YH, LEE JW, CHOİ GW, KİM HJ (2018) Risk factors and the associated cutoff values for failure of corticosteroid injection in treatment of Morton's neuroma. *Int Orthop,* 42: 323-329.

RUİZ SANTİAGO F, PRADOS OLLETA N, TOMÁS MUÑOZ P, GUZMÁN ÁLVAREZ L, MARTÍNEZ MARTÍNEZ A (2019) Short term comparison between blind and ultrasound guided injection in morton neuroma. *Eur Radiol*, 29(2): 620-627.

SANTİAGO FR, MUÑOZ PT, PRYEST P, MARTÍNEZ AM, OLLETA NP (2018) Role of imaging methods in diagnosis and treatment of Morton's neuroma. *World J RadioL,* 10: 91-99. Review.

SAMAİLA EM, AMBROSİNİ C, NEGRİ S, MALUTA T, VALENTİNİ R, MAGNAN B (2020) Can percutaneous alcoholization of Morton's neuroma with phenol by electrostimulation guidance be an alternative to surgical excision? Long-term results. *Foot Ankle Surg,* 26(3): 314-319.

SAMAİLA E, COLÒ G, RAVA A, NEGRİ S, VALENTİNİ R, FELLİ L, MAGNAN B (2021) Effectiveness of corticosteroid injections in Civinini–Morton's Syndrome: A systematic review. *Foot Ankle Surg*, 27(4): 357-365.

SATO G, FERREİRA GF, SEVİLLA D, OLİVEİRA CN, LEWİS TL, PEREİRA FİLHO MV (2022) Treatment of Morton's neuroma with minimally invasive distal metatarsal metaphyseal osteotomy (DMMO) and percutaneous release of the deep transverse metatarsal ligament (DTML): a case series with minimum two-year follow-up. *Int Orthop*, 1-7.

SHAPİRO PP, SHAPİRO SL (1995) Sonographic evaluation of interdigital neuromas. *Foot Ankle Int*, 16: 604-606.

SHARP RJ, WADE CM, HENNESSY MS, SAXBY TS (2003) The role of MRI and ultrasound imaging in Morton's neuroma and the effect of size of lesion on symptoms. *J Bone Joint Surg Br*, 85: 999-1005.

SİMMONS DN (2008) Imaging of the painful forefoot. *Tech Foot Ankle Surg*, 7: 238-249.

TERK MR, KWONG PK, SUTHAR M, HORVATH BC, COLLETTİ PM (1993) Morton neuroma: evaluation with MR imaging performed with contrast enhancement and fat suppression. *Radiology,* 189: 239-241.

UNGER HR JR, MATTOSO PQ, DRUSEN MJ, NEUMANN CH (1992) Gadopentetate-enhanced magnetic resonance imaging with fat saturation in the evaluation of Morton's neuroma. *J Foot Surg,* 31: 244-246.

VALİSENA S, PETRİ GJ, FERRERO A (2018) Treatment of Morton's neuroma: A systematic review. *Foot Ankle Surg*, 24(4): 271-281.

WAİZY H, PLAASS C, STUKENBORG-COLSMAN C (2010) Die Mortonsche Neuralgie. *Fuß & Sprunggelenk,* 8: 231-239.

WEİNFELD SB, MYERSON MS (1996) Interdigital neuritis: diagnosis and treatment. *J Am Acad Orthop Surg*, 4: 328-335.

WİLLİAMS JW, MEANEY J, WHİTEHOUSE GH, KLENERMAN L, HUSSEİN Z (1997) MRI in the investigation of Morton's neuroma: which sequences? *Clin Radiol*, 52: 46-49.

WU KK (1996) Morton's interdigital neuroma: A clinical review of its etiology, treatment andresults. *J Foot Ankle Surg*, 35: 112-119.

ZANETTİ M, LEDERMANN T, ZOLLİNGER H, HODLER J (1997a) Efficacy of MR imaging in patients suspected of having Morton's neuroma. *Am J Roentgenol*, 168: 529-532.

ZANETTİ M, STREHLE JK, ZOLLİNGER H, HODLER J (1997b) Morton neuroma and fluid in the intermetatarsal bursae on MR images of 70 asymptomatic volunteers. *Radiology*, 203: 516-520.

SUPPLEMENTARY MATERIAL

The following routine protocol for interdigital neuroma was used:

- Coronal longitudinal relaxation time-weighted (T1W) spin-echo MRI (400/12 [repetition time (ms)/echo time (ms)], 2-mm section thickness, 0.5-mm intersection space, acquisition of two signals, 12 x 6-cm field-of-view, and 572 x 262 matrix).
- Coronal STIR MRI (5373/30 [repetition time (ms)/echo time (ms)], 2-mm section thickness, 0.5-mm intersection space, acquisition of two signals, 12 x 6-cm field-of-view, and 208 x 115 matrix).
- Axial T1W spin-echo MRI (650/15 [repetition time (ms)/echo time (ms)], 2-mm section thickness, 0.3-mm intersection space, acquisition of two signals, 15 x 10-cm field-of-view, and 716 x 318 matrix).
- Coronal post- contrast SPIR (450/12 [repetition time (ms)/echo time (ms)], 2-mm section thickness, 0.5-mm intersection space, acquisition of two signals, 12 x 6-cm field-of-view, and 572 x 262 matrix).

All sequences were obtained using high resolution and with the subject in the supine position. The following MRI contrast agent was used: 0.2 mL/kg gadoterate meglumine (Dotarem, Guerbet, France).